PHYSICAL REVIEW A VOLUME 26, NUMBER 6 DECEMBER 1982

Doubly differential cross section for electron detachment from 0.5-MeV H^- in collision with He

Nasser Maleki and Joseph Macek
Department of Physics and Astronomy, University of Nebraska, Lincoln, Nebraska 68588
(Received 14 May 1982)

We calculate the energy spectrum of electrons detached from 0.5-MeV negative hydrogen ions in collision with helium targets using the plane-wave Born approximation. Three different models for continuum states of H^- are used to calculate electron-detachment doubly differential cross sections. The first model uses a single exponential function for the loosely bound electron of H^- and a plane wave for the detached electron. The second model is similar to the first one, but the final state is Gram-Schmidt orthogonalized. The third model includes the s-wave phase shifts obtained from Schwinger's variational principle. These phase shifts incorporate the radial correlations which are essential for the study of such low-energy continuum electrons. The doubly differential cross section obtained by the second and third models have a double-peak structure. These peaks are at energies different from the ones measured by Menendez and Duncan. Based on this calculation we observe that the ejected electrons are sensitive to the s-wave phase shifts and electron-electron correlations. This observation rejects the use of plane-wave models for the detached electrons and indicates the need for more accurate wave functions which incorporate radial and angular correlations.

I. INTRODUCTION

Recently Menendez and Duncan[1] (MD) in a series of experiments explored the stripping of 0.5-MeV H^- and D^- ions by He. They measured the energy distribution of doubly differential cross sections for detached electrons at several laboratory angles of ejected electrons θ_L. These experiments exhibit a sharp cusplike peak near $\theta_L \approx 0°$ with a shoulder on the low-energy side in the electron energy spectra. The sharp peak occurs at energies where the velocity of the detached electrons in the frame in which the H^- is at rest, hereafter referred to as the projectile frame, is close to zero. This peak diminishes as θ_L increases and is not visible for θ_L greater than a few degrees, whereas the lower-energy peak persists for larger θ_L. These experiments do not discriminate between detachment processes with He or H in different final states.

Upon transforming the doubly differential electron-detachment cross sections near the forward direction from the laboratory to the H^- frame we find that the energy of the observed electrons can be as low as 7 meV, even lower than the 18-meV electrons emitted in the decay of the ^1P shape resonance.[2,3] In this small energy range, 7 meV to 0.1 eV, the transition form factor of the negative hydrogen ion has some interesting structure. The purpose of this paper is to investigate the origin of such structures. One possible origin is the low-energy s-wave phase shift. By Levinson's theorem, this shift equals π at zero energy and decreases as electron energy increases. This shift in phase of the s-wave function give rise to destructive interference with higher partial waves resulting in structure in the ionization matrix elements. It is remarkable that this structure appears at an energy as low as 10 meV for the ejected electron in the H^- frame. Another possible origin of the structures in the form factors of H^- is the effect of the ^1P shape resonance of H^- in the detachment processes. We will also briefly discuss the effect of the polarization of the target atoms.

In the energy range of interest, the final s-wave function of the $e + H$ system is sensitive to the electron correlations. Accurate H^- wave functions incorporate radial and angular correlations, with the radial correlations being the most important. Thus MD's experiments provide an opportunity to test the sensitivity of the continuum H^- structure to electron correlations. In the context of plane-wave Born approximation we investigate the sensitivity of the electron spectra to radial correlations. We calculate the energy and angular distribution of doubly differential cross sections for the detached electrons in the collision of 0.5-MeV H^- with He, irrespec-

tive of the final excited state of He.

To see the relative importance of radial correlations we consider three different sets of wave functions for the H^- bound state and the adjoining continuum. Firstly, we consider a simple independent-particle ground-state function for H^- and a plane wave for the outgoing electron. Clearly this set of wave functions does not represent the system accurately because the s-wave component of the very low-energy ejected electrons has a phase shift $\delta_0 \approx \pi$ rather than the $\delta_0 = 0°$ of the plane wave. For the same reason our second choice, i.e., the first set of functions but with the plane-wave Gram-Schmidt orthogonalized to the ground-state wave function, is also not a good alternative. In this case s-wave phase shift is also 0°. Frantz, Wright, and Genoni[4] used the plane-wave orthogonalized wave functions and calculated the electron-detachment doubly differential cross sections around the forward direction for 0.5-MeV H^- on He. They found good agreement with the experimental results of MD. We also find two peaks using this second set of wave functions, nevertheless orthogonalized plane-wave functions do not represent the low-energy ejected electrons properly. Finally, for the third set we use Schwinger's variational wave functions[5] for the bound state of H^- and the s wave of the detached electron. These wave functions are obtained from one-channel close-coupling equations (with exchange) by Schwinger's variational method. Schwinger's variational phase shifts are equal to the close-coupling phase shifts[5,6] within 0.1% (see Fig. 1). Our wave functions are orthogonal, to a good approximation, and incorporate radial correlations through a qualitatively correct low-energy s-wave phase shift.

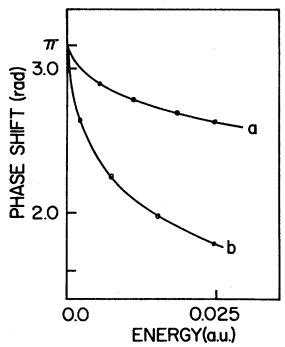

FIG. 1. Triplet (a) and singlet state (b) (static-exchange) phase shifts for electrons in the continuum of hydrogen atoms vs electron energy. Solid curves represent the values obtained by Schwinger's variational principle and circles are the values obtained by solving close-coupling equations numerically.

In Sec. II we review the relevant first Born-approximation formula. In Sec. III we list the Hartree-Fock wave functions of the He ground state, and outline the derivation of Schwinger's variational wave functions and phase shifts for the H^- system. The results are examined in Sec. IV where we study the projectile and target form factors and the electron-detachment doubly differential cross sections. We find that stripping processes which leave the He in an excited state contribute 99% of the doubly differential cross section for these low-energy electrons. Atomic units will be used throughout unless otherwise specified.

II. REVIEW OF FIRST BORN-APPROXIMATION FORMULA

When an incident atomic system "P" (projectile) with n_P electrons and nucleus of charge Z_P undergoes a fast collision with an atomic system "T" with n_T electrons and nucleus of charge Z_T, the doubly differential cross section (DDCS) for electron detachment in the first Born approximation is[7]

$$\frac{d\sigma}{k^2 dk\, d\omega} = \left[\frac{\mu^2}{4\pi^2}\right] \times \int \left[\frac{k_f}{k_i}\right] |\langle \Psi_f | V | \Psi_i \rangle|^2 d\Omega \,, \quad (1)$$

where μ is the reduced mass of the system, V is the interaction potential between P and T, $d\Omega$ and $d\omega$ are, respectively, the solid angles of scattered projectile and the ejected electron, $\vec{k}$ is the momentum of the detached electron in any inertial frame, $\vec{k}_f$ and $\vec{k}_i$ are, respectively, final and initial momentum of the projectile, and Ψ_f and Ψ_i are, respectively, the final and initial wave functions of the system. Equation (1) can be written as

$$\frac{d\sigma}{d\omega\, dE} = \left[\frac{k}{4\pi^2 v_i^2}\right] \times \int_0^{\pi} \int_{K_{\min}}^{K_{\max}} |\langle \Psi_f | V | \Psi_i \rangle|^2 K\, dK\, d\varphi \,, \quad (2)$$

where v_i is the relative velocity of the projectile and

$$\vec{K} = \vec{k}_i - \vec{k}_f \quad (3)$$

is the momentum transfer, ϕ is the azimuthal angle

of $\vec{k}_f$ in a frame with $\vec{k}_i$ along the z axis and E is the energy of the ejected electron. Since the DDCS given by Eq. (1) is invariant under Galilean transformations parallel to $\vec{k}_i$, it holds in any frame which has undergone such a transformation. We shall refer to $d^3\sigma/dk^3$ of Eq. (1) as the Galilean-invariant DDCS. Thus to write Eq. (2) in the laboratory frame, one needs to express ω and E on the left-hand side and k from the right-hand side in terms of variables given in the laboratory frame, i.e., to ω_L, and E_L and k_L, respectively. It follows from Galilean invariance that

$$\left[\frac{d\sigma}{dE\,d\omega}\right]_{\text{lab}}=\frac{k_L}{k_P}\left[\frac{d\sigma}{dE\,d\omega}\right]_{\text{proj}}, \tag{4}$$

where $\vec{k}_P$ is the momentum of the electron in the projectile frame. The laboratory cross section appears singular as the electron momentum k_P approaches zero; however, the normalization of the final-state wave function of the detached electron cancels k_P from the denominator of the right-hand side of Eq. (4). In the case of electron detachment from neutrals and positive ions the singularity is not canceled and the cross section in the laboratory frame, given by Eq. (4), becomes infinite.

Since our objective is to relate electron distributions to the structure of low-energy H^- continuum functions it is desirable to study the distribution of the detached electrons in the H^- projectile frame.[8] In the case of electron detachment from H^- in collision with He, in the H^- frame, the target (He) has an initial velocity of $-\vec{v}_i$, and initial and final momentum $-\vec{k}_i$ and $-\vec{k}_f$, respectively. The initial- and final-state wave functions of the system in the plane-wave Born approximation are

$$\Psi_i(\vec{\rho}_1,\vec{\rho}_1;\vec{r}_1,\vec{r}_2;\vec{R})=e^{i\vec{k}_i\cdot\vec{R}}\phi_i(\vec{\rho}_1,\vec{\rho}_2)\psi_i(\vec{r}_1,\vec{r}_2)\,, \tag{5}$$

and

$$\Psi_f(\vec{\rho}_1,\vec{\rho}_1;\vec{r}_1,\vec{r}_2;\vec{R})=e^{i\vec{k}_f\cdot\vec{R}}\phi_f(\vec{\rho}_1,\vec{\rho}_2)\psi_f(\vec{r}_1,\vec{r}_2)\,, \tag{6}$$

where the subscripts i and f refer to initial and final state, respectively. $\Psi(\vec{r}_1,\vec{r}_2)$ is the wave function of H^- with electron coordinate $\vec{r}_1$ and $\vec{r}_2$ in the H^- frame and $\phi(\vec{\rho}_1,\vec{\rho}_2)$ is the wave function of He with electrons at $\vec{\rho}_1$ and $\vec{\rho}_2$ in the He frame. The transition form factors for H^- and He are given by

$$\epsilon_{if}^{H^-}(K)=\langle\psi_f\,|\,(e^{i\vec{K}\cdot\vec{r}_1}+e^{i\vec{K}\cdot\vec{r}_2})\,|\,\psi_i\rangle\,, \tag{7}$$

$$\epsilon_{if}^{\text{He}}(K)=\langle\phi_f\,|\,(e^{-i\vec{K}\cdot\vec{\rho}_1}+e^{-i\vec{K}\cdot\vec{\rho}_2})\,|\,\phi_i\rangle\,. \tag{8}$$

When the He is left in the ground state

$$H^-(1s^2)+\text{He}(1s^2)\rightarrow\text{H}(1s)+e^-+\text{He}(1s^2)\,, \tag{9}$$

we have[9]

$$\frac{d\sigma}{dE\,d\omega}=(4k/v_i^2)\int_0^{2\pi}\int_{K_{1\min}}^{K_{1\max}}|\epsilon_{if}^{H^-}|^2\,|\,2-\epsilon_{00}^{\text{He}}\,|^2\frac{dK}{K^3}d\varphi_{\text{He}}\,, \tag{10}$$

where

$$K_{1\max}=k_{1f}+k_i,\quad K_{1\min}=k_{1f}-k_i\,, \tag{11}$$

k_{1f} is the final momentum of the projectile, I_{H^-} is the ionization potential of H^- and k denotes the momentum of the detached electron in the H^- frame. The sum of all processes in which the target is excited or ionized, i.e.,

$$H^-(1s^2)+\text{He}(1s^2)\rightarrow\text{H}(1s)+e^-+\text{He}^* \tag{12}$$

is approximately given by[9]

$$\frac{d\sigma}{dE\,d\omega}=(4k/v_i^2)\times\int_0^{2\pi}\int_{K_{2\min}}^{K_{2\max}}|\epsilon_{if}^{H^-}|^2(4-|\epsilon_{00}^{\text{He}}|^2)\times\frac{dK}{K^3}d\varphi_{\text{He}}\,, \tag{13}$$

where

$$K_{2\max}=k_{2f}+k_i\,,$$
$$K_{2\min}=[k^2+2(I_{H^-}+I'_{\text{He}})]/2v_i\,, \tag{14}$$

k_{2f} is the final momentum of the projectile, and I'_{He} is the average excitation energy of He.

III. WAVE FUNCTIONS

In the collision of 0.5-MeV H^- with He the electron-detachment doubly differential cross section is not very sensitive to the wave functions of He. In the last section we showed that for processes leaving He in an excited state the doubly differential cross section can be written in terms of the form factors of H^- and He in its ground state. We

will use Hartree-Fock wave functions[10]

$$\phi_0^{\mathrm{HF}}(\vec{\rho}_1,\vec{\rho}_2)=\mathcal{K}(\vec{\rho}_1)\mathcal{K}(\vec{\rho}_2) \tag{15}$$

for the helium ground state. In Eq. (13)

$$\mathcal{K}(\vec{\rho})=(a_1e^{-a_2\rho}+b_1e^{-b_2\rho})Y_{00}(\hat{\rho}) \tag{16}$$

with

$$\begin{aligned} &a_1=2.605\,05,\quad a_2=1.41\ , \\ &b_1=2.081\,44,\quad b_2=2.61\ . \end{aligned} \tag{17}$$

This wave function is sufficiently accurate for the processes under investigation. Conversely, wave functions of H^- are very crucial to the calculation of electron-detachment DDCS in the energy range of interest. We use

$$\psi_i(\vec{r}_1,\vec{r}_2)=[\phi_{1s}(\vec{r}_1)\psi_g(\vec{r}_2)+\phi_{1s}(\vec{r}_2)\psi_g(\vec{r}_1)]/N \tag{18}$$

for the initial H^- wave function and

$$\psi_f(\vec{r}_1,\vec{r}_2)=[\phi_{1s}(\vec{r}_1)\psi_{\vec{k}}^{-}(\vec{r}_2)+\phi_{1s}(\vec{r}_2)\psi_{\vec{k}}^{-}(\vec{r}_1)]/\sqrt{2} \tag{19}$$

for the final $e^-+\mathrm{H}$ wave functions, where ϕ_{1s} is the ground-state hydrogen wave function, ψ_g is the H^- bound-state wave function, N is a normalization constant and $\psi_{\vec{k}}^{-}$ is the wave function of the ejected electron with energy $E=k^2/2$.

To investigate radial correlations we choose three different ψ_g and $\psi_{\vec{k}}^{-}$. First we use[11]

$$\psi_g(r)=e^{-0.28r} \tag{20}$$

and

$$\psi_{\vec{k}}(r)=(2\pi)^{-3/2}e^{i\vec{k}\cdot\vec{r}}\ . \tag{21}$$

These functions incorporate no electron correlations. Frantz, Wright, and Genoni[4] applied the Gram-Schmidt orthogonalization procedure to this set of wave functions and calculated electron-detachment DDCS for process (12). We used these orthogonalized plane-wave functions for our second set of wave functions. These functions also do not include any electron correlation, but are orthogonal. Next we use a partial-wave expansion of $\psi_{\vec{k}}$, i.e.,

$$\psi_{\vec{k}}(\vec{r})=(2\pi)^{-3/2}\sum_{l=0}^{\infty}(2l+1)\exp(i\delta_l)\times(i)^l u_l(r)P_l(\cos\theta)\ . \tag{22}$$

Since $\delta_l\simeq 0$ for $l\neq 0$ for very low-energy electrons, we approximated

$$u_l(r)=j_l(kr),\quad l>0 \tag{23}$$

where $j_l(kr)$ is a spherical Bessel function of lth order. Equations (22) and (23) give

$$\begin{aligned} \psi_{\vec{k}}^{-}(\vec{r})=&\pi^{-1}(2)^{-1/2}\exp(-i\delta_0)u_0(r)Y_{00}(\hat{r}) \\ &-\pi^{-1}(2)^{-1/2}j_0(kr)Y_{00}(\hat{r}) \\ &+(2\pi)^{-3/2}e^{i\vec{k}\cdot\vec{r}} \end{aligned} \tag{24}$$

which is normalized per unit momentum. In Eq. (24) δ_0 is the s-wave phase shift and $u_0(r)$ is the s-wave function with the radial correlation incorporated. To obtain a reliable closed-form expression for u_0 we use Schwinger's variational principle. These wave functions, to a good approximation, are equal to the ones obtained by numerical integration of the close-coupling equations.[5]

Equation (L65) of Ref. 12, the integro-differential equation for the scattering of electrons by hydrogen atoms in the Hartree-Fock approximation, reads[12]

$$\left[\frac{d^2}{dr_1^2}-\frac{l(l+1)}{r_1^2}-W(r_1)+k^2\right]F_l(r_1)=\pm\left[\frac{8\pi}{2l+1}\int_0^{\infty}\frac{r_<^l}{r_>^{l+1}}F_l(r_2)\phi_{1s}(r_2)r_2dr_2 - 4\pi(1+k^2)\delta_{l0}(1+k^2)\int_0^{\infty}F_l(r_2)\phi_{1s}(r_2)r_2dr_2\right]r_1\phi_{1s}(r_1)\ , \tag{25}$$

where δ_{l0} is the Kronecker delta function and

$$W(r)=-2(1+1/r)e^{-2r}\ . \tag{26}$$

Equation (25) has the operator form

$$(h_l-E)\,|F_l\rangle=-V\,|F_l\rangle\ , \tag{27}$$

where

$$h_l=-\frac{1}{2}\left[\frac{d^2}{dr^2}-\frac{l(l+1)}{r^2}\right], \tag{28}$$

$$E=k^2/2, \tag{29}$$

and

$$V(r_1,r_2)=\pm\frac{1}{2}\left[\frac{8\pi}{2l+1}\frac{r_<^l}{r_>^{l+1}}\phi_{1s}(r_2)-4\pi(1+k^2)\phi_{1s}(r_2)\delta_{l0}\right]\phi_{1s}(r_1)-\left[1+\frac{1}{r^2}\right]e^{-2r_2}\delta(r_1-r_2)\,. \tag{30}$$

Schwinger's variational phase shifts and wave functions for the e^- + H system are given by[5,6]

$$k\cot\delta_l=-\langle F_t\,|\,(V+VG^PV)\,|\,F_t\rangle/|\langle F_t\,|\,V\,|\,f_l\rangle\,|^2, \tag{31}$$

$$|\,u_l\rangle=|\,f_l\rangle+\tan(\delta_l)G^PV\,|\,F_t\rangle/\langle F_t\,|\,V\,|\,f_l\rangle\,. \tag{32}$$

The wave function for the bound state of H^-, i.e., ψ_g is

$$|\,\psi_g\rangle=-G_bV\,|\,F_t\rangle, \tag{33}$$

where G^P is the principal part of the free Green's function

$$f_l(r)=j_l(kr), \tag{34}$$

and G_b is the analytical continuation of G to the negative-energy region, i.e., where $\kappa^2/2$ is the ionization potential of H^-.

In Eqs. (31), (32), and (33) F_t's are trial functions which are only required to be accurate in the region where $V\neq0$ (Ref. 6); when one trial function (for $l=0$),

$$F_t(r)=e^{-br},\quad b=0.47, \tag{35}$$

is used, good agreement with the results of numerical integration of Eq. (25) is achieved, as shown in Fig. 1.

The s-wave phase shifts obtained by this variational method are accurately given by the effective-range formula

$$k\cot\delta_0=-\frac{1}{a}+\left[\frac{r_0}{2}\right]k^2\,. \tag{36}$$

The scattering length a and effective range r_0 are found to be

$$a=8.06,\quad r_0=3.02\,. \tag{37}$$

We have used these values of a and r_0 to obtain $\kappa^2=0.028$ a.u. for the bound-state energy of H^-. These results agree within 0.1% with those obtained by direct numerical integration of Eq. (25).[5,12]

Our explicit expression for the continuum s-wave function, Eq. (32), and the bound-state wave function of H^-, Eq. (33), are given by

$$u_0(r)=(kr)^{-1}\sin(kr+\delta_0)+k^{-1}\sin\delta_0P^c(r) \tag{38}$$

and

$$\psi_g(r)=r^{-1}e^{-\kappa r}+P^0(r), \tag{39}$$

where

$$P^c(r)=-r^{-1}\exp[-(b+2)r]+a_1^c\exp[-(b+2)r]+a_2^ce^{-r} \tag{40}$$

and

$$P_b^c(r)=-r^{-1}\exp[-(b+2)r]+a_1^b\exp[-(b+2)r]+a_2^be^{-r}\,. \tag{41}$$

The coefficients in $P^c(r)$ and $P^b(r)$ are

$$a_1^b=-0.4884,\quad a_2^b=-1.3097 \tag{42}$$

and

$$a_1^c=-0.4893-0.0318k^2,\qquad a_2^c=-1.3184-0.1k^2, \tag{43}$$

to order k^4.

Equations (42) and (43) indicate that $P^b(r)$ and $P^c(r)$ for most practical purposes can be considered equal for $k^2<0.1$ a.u. Equation (38) for $u_0(r)$ is designed so that the incoming electron wave has correct asymptotic behavior, that is,

$$u_0(r)\underset{r\to\infty}{\sim}(kr)^{-1}\sin(kr+\delta_0)\,. \tag{44}$$

The wave functions evaluated by this method are also in good agreement with the ones obtained by numerical integration of Eq. (25). Clearly the initial state of H^- and the final state of the e + H system constructed from the exact numerical functions are orthogonal. Thus the agreement between the Schwinger's variational and the numerical wave

function establishes, to a good approximation, the orthogonality of our initial and final states. These wave functions do not, however, take into account any angular correlations. We used the three sets of wave functions, given in this section, to investigate electron-detachment DDCS from 0.5-MeV H^- in the collision with He. Such processes are studied in the next section, first by considering H^- and He form factors as a function of momentum transfer and then examining the sensitivity of DDCS to s-wave phase shifts.

IV. RESULTS

In this section we evaluate the target transition form factors and show that DDCS for process (12) overwhelms the contribution from process (9). Then we study H^- form factors and electron-detachment DDCS evaluated using the three different sets of H^- wave functions discussed in Sec. III.

We have evaluated the DDCS using Eqs. (10) and (13) and find that processes in which the He is excited [Eq. (12)] dominate in the energy region of interest. To see how this arises note that Eqs. (10) and (13) suggest that for the low-energy detached electrons the ratio

$$R_T=(Z_T^2-|\epsilon_{00}^T|^2)/|Z_T-\epsilon_{00}^T|^2 \tag{45}$$

is a measure of the relative contribution to electron detachment DDCS from processes leaving the target in the ground state as compared to processes leaving the target in any excited state. In the case of the He atom as target we use Hartree-Fock wave functions given by Eq. (15) for calculation of $\epsilon_{00}^{\mathrm{He}}$. Simple integration leads to

$$\epsilon_{00}^{\mathrm{He}}(K)=2\left[\frac{4a_2a_1}{(4a_2^2+K^2)^2}+\frac{4b_2b_1}{(4b_2^2+K^2)^2}+\frac{4a_1b_1(a_2+b_2)}{[(a_2+b_2)^2+K^2]^2}\right]. \tag{46}$$

For all values of K this form is in excellent agreement with the form factor obtained from the 20-term Hylleras wave function.[13] Since K is small we expand ϵ_{00}^T around zero momentum transfer and retain only the terms up to K^2 order;

$$\epsilon_{00}^T(K)\simeq Z_T-CK^2\,, \tag{47}$$

where C is a constant which depends on the target, for example, for hydrogen $C=0.5$ and for helium $C=0.3946$. Substitution of ϵ_{00}^T from Eq. (47) into Eq. (45) gives

$$R_T=2Z_T/CK^2 \tag{48}$$

which is a large number in the region of small momentum transfer.

Since $R_T\gg1$ we calculate DDCS using Eq. (13). This equation can be put into a more convenient form by substitution of $\epsilon_{00}^{\mathrm{He}}$ from Eq. (47); we obtain

$$\frac{d\sigma}{dE\,d\omega}\simeq\frac{16kC}{v_i^2}\int_0^{2\pi}\int_{K_{2\min}}^{K_{2\max}}|\epsilon_{00}^{H^-}|^2 d[\ln(K)]d\varphi_{\mathrm{He}}=\int_{K_{2\min}}^{K_{2\max}}J(K)d[\ln(K)]\,, \tag{49}$$

where

$$J(K)\equiv\frac{16kC}{v_i^2}\int_0^{2\pi}|\epsilon_{00}^{H^-}|^2 d\varphi_{\mathrm{He}}\,. \tag{50}$$

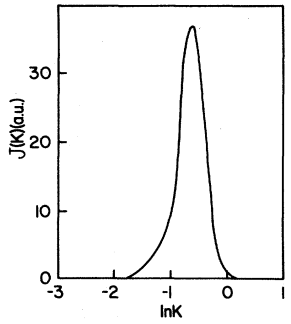

FIG. 2. $J(K)$ vs $\ln K$ in the laboratory frame with initial and final states of H^- constructed by Schwinger's variational s-wave functions. Area under the curve is the DDCS for electron detachment from 0.5-MeV H^- in the collision with He for $\theta_L=0.3°$ and $k_L=4.43$ a.u.

In Fig. 2 $J(K)$ is plotted versus $\ln K$ for $k_L=4.43$

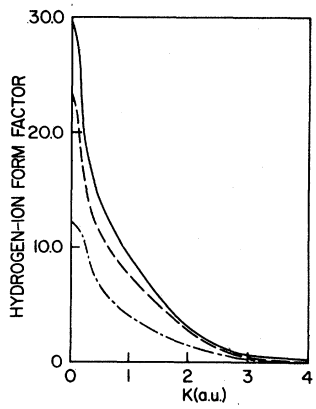

FIG. 3. $\epsilon_{00}^{H^-}$ vs K, where $j_0(kr)$ and $e^{-0.28r}$ are used for ψ_g and $\psi_{\vec{k}}$. Solid, dashed, and dot-dashed curves are for $k=0.05$, 0.1, and 0.2 a.u., respectively.

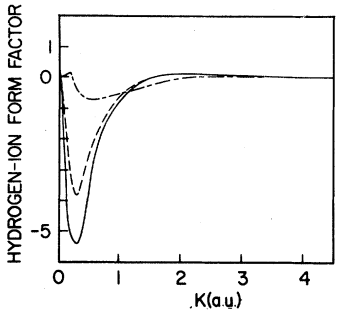

FIG. 4. $\epsilon_{00}^{H^-}$ vs K, where $j_0(kr)$ and $e^{-0.24r}$ are used for $\psi_{\vec{k}}$ and ψ_g with ψ_f and ψ_i Gram-Schmidt orthogonalized. (See caption of Fig. 3 for identification of curves.)

using the third set of wave functions. The area under this curve gives the DDCS for process leaving the target in an excited state. Note that since $\ln K_{2\min}$ is of the order of -1.6 where $J(K)$ is small, the integral in Eq. (50) is insensitive to the lower limit of integration.

Figures 3—13 contain the plots of H^- form factors and DDCS for 0.5-MeV H^- $1s^2$ on the He $1s^2$ target. In order to clarify the importance of the s-wave phase shifts we also use $j_0(kr)$ for u_0 and $e^{-0.28r}$ for ψ_g. The corresponding form factors $\epsilon_{00}^{H^-}(K)$ are plotted in Fig. 3. The large value at $K=0$ suggests the need for better ψ_g, ψ_k, and the orthogonality of ψ_i and ψ_f. With the Gram-Schmidt-orthogonalized final free s-wave function, the s-wave form factor as shown in Fig. 4 improves significantly for low momentum transfer and small electron energies, but it goes through two zeros for higher electron energies. The zeros in the form factors are due to the orthogonalization and have no apparent physical basis.

Figure 5 shows the s-wave form factors obtained using Schwinger's variational functions for ψ_g and $\psi_{\vec{k}}$. the approximate orthogonality of ψ_i and ψ_f is apparent from Fig. 5. Comparison of Figs. 4 and 5

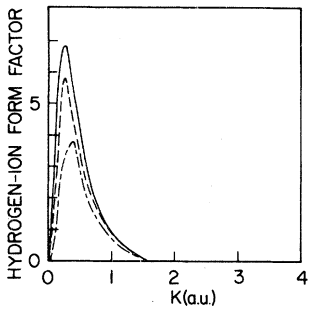

FIG. 5. s-wave $\epsilon_{00}^{H^-}$ plotted vs K, where Schwinger's s-wave functions given in Sec. II are used for ψ_g and $\psi_{\vec{k}}$. (See caption of Fig. 3 for identification of curves.)

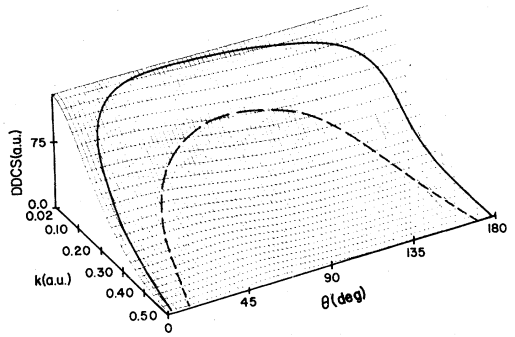

FIG. 6. Galilean-invariant DDCS in the projectile frame vs k and θ, with $\psi_{\vec{k}}=(2\pi)^{-3/2}e^{i\vec{k}\cdot\vec{r}}$ and $\psi_g=e^{-0.28r}$. Solid and dashed curves on the surface sample electron energies from the laboratory frame for $\theta_L=0.3°$ and 1.5°, respectively.

indicates distinct differences due to incorporation of radial correlation through the s-wave phase shifts by Schwinger's variational functions. The s-wave form factors obtained by Schwinger's variational functions differ in sign from those obtained using the orthogonalization procedure. This difference in sign is partially compensated by the $\exp(-i\delta_0)$ factor in the partial-wave expansion given by Eq. (24). These more accurate form factors are sharply peaked, concentrated near smaller K, and are smooth functions of electron energy in contrast to those of Fig. 4.

To see the importance of the other partial waves relative to the s-wave we include higher partial waves as in Eq. (24). Using this set of wave functions we calculated

$$\langle \epsilon_{00}^{H^-}(K)\rangle_{\varphi_{He}} \equiv \left[\int_0^{2\pi} |\epsilon_{00}^{H^-}|^2 d\varphi_{He}\right]^{1/2}/2\pi \qquad (51)$$

which is the H^- form factor averaged over the azimuthal angle of the projectile. We find that al-

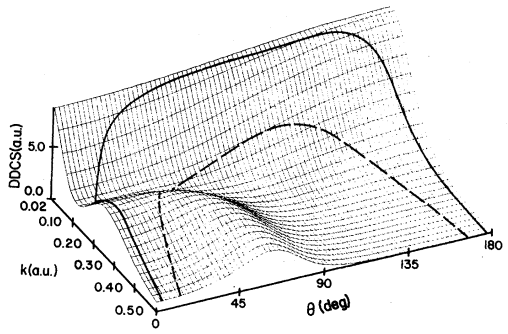

FIG. 7. Galilean-invariant DDCS in the projectile frame vs k and θ with $\psi_{\vec{k}}=(2\pi)^{-3/2}e^{i\vec{k}\cdot\vec{r}}$ and $\psi_g=e^{-0.28r}$ where ψ_f and ψ_i are Gram-Schmidt orthogonalized. (See caption of Fig. 6 for identification of the solid and dashed curves.)

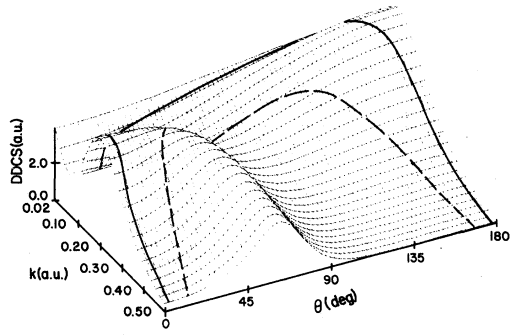

FIG. 8. Galilean-invariant DDCS in the projectile frame vs k and θ, where Schwinger's s-wave functions are used for ψ_g and in partial-wave expansion of $\psi_{\vec{k}}$. (See caption of Fig. 6 for identification of the solid and dashed curves.)

though the s wave is the most important partial wave in this calculation, the contribution due to the higher partial waves is not negligible. Because the higher-partial-wave phase shifts can be practically set equal to zero, our results imply that the electron radial correlations are adequately incorporated through phase-shifted s waves for small electron energies.

Figure 6—8 show the Galilean-invariant DDCS for electron detachment versus k and θ in the H^- frame where θ is the electron-ejection angle in the H^- frame, that is, the angle between $\vec{k}$ and $-\vec{v}$. From

$$\vec{k}_L=\vec{k}+\vec{v}_i \tag{52}$$

we have

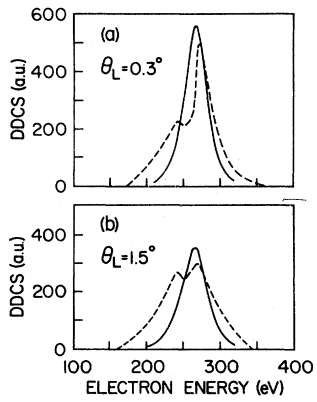

FIG. 9. Laboratory-frame DDCS for electron detachment of H^- vs detached-electron energies with the plane-wave model. Parts (a) and (b) are for $\theta_L=0.3°$ and 1.5°, respectively. Solid curves are the results of this calculation and the dashed curves are experimental results of Menendez and Duncan.

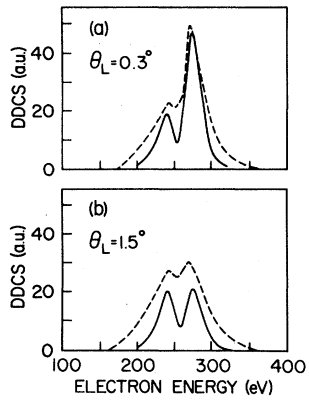

FIG. 10. Same as Fig. 9, but the final plane-wave function is Gram-Schmidt orthogonalized to the initial state.

$$k^2=k_L^2+v_i^2-2k_Lv_i\cos\theta_L \tag{53}$$

and

$$\cos\theta=(k_L\cos\theta_L-v_i)/k\ . \tag{54}$$

At fixed ejection angle, say $\theta_L=0.3$ or 1.5, the electron energy in the laboratory frame $\frac{1}{2}k_i^2$ samples the two-dimensional surface of Figs. 6—8 at a series of points along a curve determined by Eqs. (53) and (54). The solid and dashed curves trace the laboratory electron energies for $\theta_L=0.3°$ and 1.5°, respectively. The peak in the laboratory frame occurs at those points along the curves where DDCS goes through a maxima.

For Fig. 6 we use the first set of wave functions given in Sec. III. It is clear that the first approximation gives only one maximum which corresponds

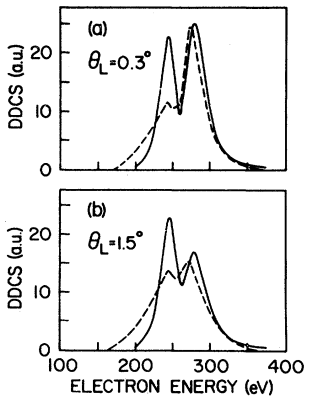

FIG. 11. Laboratory-frame DDCS for electron detachment of H^- vs detached-electron energies, with Schwinger's variational s-wave functions used for ψ_g and in partial-wave expansion of $\psi_{\vec{k}}$. Parts (a) and (b) are, respectively, for $\theta_L=0.3°$ and 1.5°. (See caption of Fig. 9 for identification of the solid and dashed curves.)

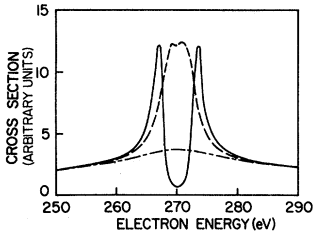

FIG. 12. Laboratory-frame ^1P shape resonance cross section of H^- vs electron energies in the laboratory frame. Solid curve for $\theta_L=0.3°$, dashed curve for $\theta_L=0.45°$, and dot-dashed curve for $\theta_L=0.85°$.

to the smallest electron velocity $V_e=4.47$ a.u. in the H^- frame. Figure 7 has an extra maximum due to the orthogonalization of the second set of wave functions, which has no apparent physical basis. For the results in Fig. 8, the third set of wave functions are used, that is, incorporated the Schwinger's variational s-wave functions in a partial-wave expansion of $\psi_{\vec{k}}^{-}$ for the ejected electron. This figure shows a double-peak structure in DDCS which corresponds to a double peak in the laboratory frame at electron energies of 262 and 295 eV for $\theta_L=0.3°$ and 1.5°.

Figures 9—11 show the DDCS versus detached electron energies in the laboratory frame at $\theta_L=0.3°$ and 1.5°. For comparison, the experimental results of Menendez and Duncan[1] are also plotted. These data are scaled to have the same order of magnitude as the calculated DDCS. Figure 9 is obtained by the first set of wave functions. This figure has only one maximum, as predicted by Fig. 6, in disagreement with the experimental results. The maximum occurs approximately at the electron-projectile velocity matching point, i.e., $v_E\approx v_i=4.47$ a.u.

With the second set of wave functions the calculated DDCS in Fig. 10 has peaks at 250 and 274 eV as shown by the experiments and the calculation of

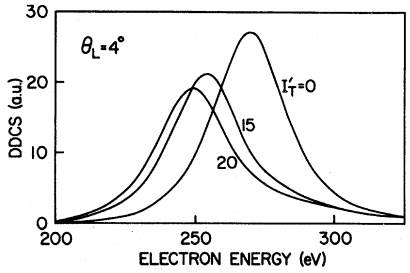

FIG. 13. Laboratory-frame DDCS for electron detachment of H^- vs detached-electron energy with $\theta_L=4°$ and $I_T'=0$, 15, and 20 eV. Schwinger's variational s-wave functions are used for ψ_g and in a partial-wave expansion of $\psi_{\vec{k}}^{-}$.

Franz, Wright, and Genoni.[4] This apparently fortuitous agreement is due to destructive interference between the s-wave component and the higher-partial-wave components of the transition form factor of H^-. The physical basis of such interference is the phase shift of the s partial wave which is consistently treated with the third set of wave functions. The DDCS of Fig. 11 are obtained using this set of wave functions. They have a double-peak structure as predicted by Fig. 8; however, the position of the peaks (244 and 278 eV for $\theta_L=0.3°$, 246, and 278 eV for $\theta_L=1.5°$) are not in agreement with experiment and their magnitudes do not have the same sensitivity to θ_L as in the experiments. These results are very sensitive to the s-wave phase shifts which incorporate radial correlations only. Thus the forward-angle DDCS could provide a sensitive test of the electron-electron correlations for loosely bound system such as H^-. In the rest of this section we will discuss two additional factors which may affect the magnitude and the positions of the maxima in DDCS, that is, the decay of the ^1P shape resonance of H^- and the polarizability of the target atom.

Our results in Fig. 11 do not show a sharp peak at 0.3° which disappears at 1.5°, in contrast to the experimental results. Furthermore, the minimum between the peaks in experimental curves is much less pronounced than in any of the calculations. We have noted, however, that the electron energy in the H^- frame is as low as 7 meV for $\theta_L=0.3°$, which is lower than the energy of 18-meV electrons from the decay of the doubly excited ^1P shape resonance of H^-. This resonance could contribute to DDCS at 0.3° but not at 1.5°. We investigate its contribution phenomenologically by using the Breit-Wigner formula to model the resonance contribution. We have in the H^- frame

$$\sigma(E)\propto\frac{\Gamma/2}{(E-E_r)^2+(\Gamma/2)^2}\ , \tag{55}$$

where E is the electron energy in H frame, Γ_r and E_r are, respectively, resonance width and energy, with[2,3] values $E_r=18$ meV and $\Gamma_r=85.4$ meV. We have actually taken $\Gamma_r=k^3\gamma$, where γ is a constant in accord with the argument of Macek.[2] The results are plotted versus electron energy in the laboratory frame in Fig. 12 for $\theta_L=0.3°$, 0.45°, and 0.85°. For $\theta_L=0.3°$ there is a double peak around 270 eV but when θ_L is increased by 0.15°, $d\sigma$ has one single peak. As θ_L increases, this peak, which is at 272 eV, vanishes. More precisely the resonance disappears at about $\theta_L=0.85°$. Comparison of Fig. 12 with the experimental data in Figs. 9—11 shows

that the behavior of the resonance cross section is similar to the behavior of the sharp peak at 272 eV in the experimental DDCS for electron detachment. This suggests the possibility of a ^1P shape resonance contribution in the electron-detachment processes. Since the ^1P resonance decays predominantly to the $n=2$ state of hydrogen, detection of the secondary electrons in coincidence with Lyman-α photons would provide a more definitive test of this hypothesis.

In Fig. 11 the slopes of the low-energy shoulder of DDCS are different from the slopes predicted by the experiments. Since this laboratory energy region corresponds to $k^2 > 0.09$ a.u. where the p-wave phase shifts become important,[12] the disagreement may be due to the absence of p-wave phase shifts in our calculation.

The angular distribution of the detached electron from H^- in the collison with Ar or He at large angle can be approximated by the angular distribution of elastic scattering of electrons from Ar or He.[14] Here, the polarization of the target affects the scattered-electron distribution in the forward direction.[15] Hence, the dynamic dipole interaction in detachment collisions of H^- from He influences the angular distribution of the ejected electrons. Some evidence for this is provided by the observation of a target dependence in the DDCS for H^- stripping. We have seen that the DDCS is almost independent of the target structure except through $K_{\min}$ which depends on the average ionization energy I_T' of the target. To examine this dependence we have calculated the DDCS at $\theta_L = 4°$ for $I_T' = 0$, 15, and 20 eV. We see in Fig. 13 that the peak shifts toward higher energies as I_T' decreases. Now $I_T' = 0$ corresponds to stripping by a target with a permanent dipole moment, thus a peak shift may indicate the influence of an induced dipole moment in the target. Such an effect is not incorporated in the first Born approximation considered here.

V. CONCLUSIONS

In the context of the plane-wave Born approximation three models for $e^- + H$ system are used to calculate electron-detachment DDCS from 0.5-MeV H^- in collision with He. The first two models, namely, plane waves and orthogonalized plane waves for the detached electron are not satisfactory due to the very low energy of the detached electrons. Our third choice of the $e^- + H$ wave function incorporates radial correlations through the s-wave functions of the detached electrons, which are obtained by Schwinger's variational principle. Angular correlations are neglected in this calculation. The DDCS obtained by the third set of wave functions are sensitive to the s-wave phase shifts and have the double-peak structure. These peaks do not have the same sensitivity to θ_L as in the experiments of Menendez and Duncan and their positions do not agree with experiments. These results also show that, although the s waves are the most important for such calculations, the effect of other partial waves is not negligible; our calculations suggest the need for a more accurate set of $e + H$ wave functions, that is, wave functions which treat angular correlations as well.

Independent of projectile structure we showed that the excitation of the target has an overwhelming effect on the magnitude of the DDCS's in the detached-electron energy region under consideration. Since the polarization of the He in the detachment process is not negligible, the dynamic dipole interaction may influence the angular distribution of the detached electrons and could enhance processes in which the target is left in the ground state. We have also examined the contribution of the ^1P shape resonance of H^- phenomenologically. The peak in the DDCS for this resonance vanishes by increasing the laboratory detection angle of the detached electron. This behavior is similar to the behavior of the large peak in Menendez and Duncan's experimental results.

ACKNOWLEDGMENT

This work was supported by the National Science Foundation under Grant No. PHY-8203400.

[1]M. G. Menendez and M. M. Duncan, Phys. Rev. A 20, 2327 (1979).
[2]J. Macek, Proc. Phys. Soc. London 92, 365 (1967).
[3]H. C. Bryant *et al.*, Phys. Rev. Lett. 5, 228 (1977).
[4]M. R. Franz, L. A. Wright, and T. C. Genoni, Phys. Rev. A 24, 1135 (1981).
[5]N. Maleki, Ph.D. thesis, University of Nebraska, 1981 (unpublished).
[6]N. Maleki and J. Macek, Phys. Rev. A 21, 1403 (1980).
[7]N. F. Mott and H. S. W. Massey, *Theory of Atomic Col-*

lisions (Clarendon, Oxford, 1949), Chap. VIII.
[8]F. Drepper and J. S. Briggs, J. Phys. B 9, 2063 (1976).
[9]*Topics in Current Physics,* edited by J. A. Sellin (Springer, Berlin and Heidelberg, 1978), Vol. 5, p. 105.
[10]E. Clementi and C. Roetti, At. Data Nucl. Data Tables 14, 177 (1974).
[11]H. A. Bethe and E. E. Salpeter, *Quantum Mechanics of One- and Two-Electron Atoms* (Plenum, New York, 1977), Sec. 34.
[12]T. Y. Wu and T. Ohmura, *Quantum Theory of Scattering* (Prentice-Hall, Englewood Cliffs, New Jersey, 1962).
[13]Y. K. Kim and M. Inokuti, Phys. Rev. 165, 39 (1968).
[14]H. G. Menendez and M. M. Duncan, Phys. Rev. Lett. 40, 1642 (1978).
[15]K. W. LaBahn and J. Callaway, Phys. Rev. 180, 91 (1961).